doi: 10.18323/2782-4039-2024-4-70-6

Electrochemical interaction between biodegradable ZX10 and WZ31 magnesium alloys and medical Ti6Al4V titanium alloy

Pavel N. Myagkikh*[1], PhD (Engineering),
junior researcher of the Research Institute of Advanced Technologies
Evgeny D. Merson[2], PhD (Physics and Mathematics),
senior researcher of the Research Institute of Advanced Technologies
Vitaly A. Poluyanov[3], PhD (Engineering),
junior researcher of the Research Institute of Advanced Technologies
Dmitry L. Merson[4], Doctor of Sciences (Physics and Mathematics),
Professor, Director of the Research Institute of Advanced Technologies
Marina E. Begun, student,
technician of the Research Institute of Advanced Technologies
Togliatti State University, Togliatti (Russia)

***E-mail:** p.myagkikh@tltsu.ru

[1]ORCID: https://orcid.org/0000-0002-7530-9518
[2]ORCID: https://orcid.org/0000-0002-7063-088X
[3]ORCID: https://orcid.org/0000-0002-0570-2584
[4]ORCID: https://orcid.org/0000-0001-5006-4115

Received 08.05.2024 *Revised 09.10.2024* *Accepted 07.11.2024*

Abstract: Magnesium-based alloys are a modern material for the production of biodegradable (self-dissolving) surgical implants. Magnesium is a metal with the most negative electrode potential of all structural materials: −2.37 V. This means that close arrangement of implants made of magnesium, and for example, titanium alloys will lead to the occurrence of a galvanic effect, and accelerated electrochemical corrosion of magnesium. However, it is unknown how the ratio of the areas of titanium and magnesium products affects the magnitude of this effect. This work covers this issue. In the presented study, cylindrical samples of biodegradable ZX10 and WZ31 magnesium alloys were placed in physiological Ringer's solution at a distance of 3 cm, from a sample of medical Ti6Al4V alloy of the same shape and size. During the test, the temperature of the corrosive environment was maintained at 37 °C. The series of experiments included corrosion tests lasting three days with the participation of one, two or four magnesium samples, thus the area ratios between the titanium and magnesium alloy were 1:1, 1:2 and 1:4. It was found that for both magnesium alloys, with an increase in the area ratio, the effect of electrochemical action decreases significantly, which is expressed in a decrease in the corrosion rate. At the same time, for the WZ31 alloy, the effect of the presence of Ti6Al4V on the corrosion rate is significantly weaker than for ZX10, which is explained by the presence of the LPSO phase in the alloy, as well as a more alloyed matrix and, accordingly, having a more positive electrode potential.

Keywords: surgical implants; electrochemical corrosion; biodegradable materials; magnesium alloys; ZX10; WZ31; titanium alloys; Ti6Al4V; medical materials; corrosion rate; electrode potential.

Acknowledgments: The research was financially supported by the Russian Science Foundation, project No. 23-23-10041 (https://rscf.ru/project/23-23-10041/), project No. 23-19-00636 (https://rscf.ru/project/23-19-00636/).

For citation: Myagkikh P.N., Merson E.D., Poluyanov V.A., Merson D.L., Begun M.E. Electrochemical interaction between biodegradable ZX10 and WZ31 magnesium alloys and medical Ti6Al4V titanium alloy. *Frontier Materials & Technologies*, 2024, no. 4, pp. 63–71. DOI: 10.18323/2782-4039-2024-4-70-6.

INTRODUCTION

The idea of a self-dissolving surgical implant for osteosynthesis has long been under close attention of scientists and medical companies. Such implants do not require an operation to remove them, which is a serious stress for the patient's body. One of the simplest solutions is the use of bioresorbable polymers such as polylactide, polydopamine, polycaprolactone, etc. Indeed, these materials are quite cheap and easy to process. At the same time, the strength properties of polymers cannot be compared with metals. Attempts to solve the problem, for example, by creating a polymer-metal composite [1], continue, but significant progress has not yet been achieved. Similar problems are observed for bioresorbable ceramics, which are also much more fragile. Among the metallic materials, iron, zinc and magnesium are considered as a basis for bioresorbable alloys [2], some researchers consider tungsten [3; 4], and metallic glasses based on calcium, zinc and strontium [5] as a bioresorbable material. Magnesium alloys

are already used for the commercial manufacturing of medical self-dissolving products; moreover, the Young's modulus of magnesium of the presented elements is the closest to that of bone, which is also an important factor, since an implant made of such a material is capable of elastic deformation, in concert with the bone.

The operating conditions of a magnesium alloy implant can directly affect its characteristics, such as the corrosion rate. For example, a titanium implant may already be installed in the immediate proximity to the installation site of a magnesium alloy medical device. It is known that due to the lowest electrode potential among all structural materials, magnesium is prone to electrochemical corrosion in the presence of other metals [6; 7], because of the formation of a galvanic couple between the more negative magnesium, and the more positive metal. In [8], using Kelvin probe atomic force microscopy, evidence was obtained that in some cases, even the corrosion products appearing on the surface of a magnesium alloy, can have a more positive potential and are capable of forming a galvanic couple with the magnesium matrix. In [9], where magnesium alloys doped with silver were studied, it was demonstrated that with the addition of silver, the corrosion properties first improve, and then the corrosion resistance drops sharply. The authors attribute this to the difference in electrode potential between the matrix, and the intermetallic particles released upon reaching the solubility limit of the ligature. However, except for the electrode potential, there are a number of other factors affecting electrochemical corrosion. The most important of these is the distance at which the galvanic effect between magnesium and another metal will have a significant effect on the corrosion rate.

In [10], a magnesium screw was installed directly into a titanium plate (i.e., had direct contact with it) secured, in addition to it, by titanium screws. Based on the results of experiments, including *in vivo* tests on rabbits, the authors note that the magnesium screw contributed to the formation of enlarged callus, and accelerated its mineralization compared to the control group, where only titanium screws were used to attach the titanium plate. At the same time, in the X-ray images presented in this work, the magnesium screw is almost invisible already three weeks after the operation. This indicates that in just 21 days it almost completely dissolved under the influence of the aggressive environment of a living organism and electrochemical interaction with the titanium plate and screws. Obviously, the intensive dissolution of the screw accelerated the formation of bone callus, due to the enrichment of tissues with magnesium. However, at the same time, one should note that the screw itself dissolved too quickly. In the scheme proposed by the authors, where several titanium screws bear the main load, such a dissolution rate is acceptable. However, if we talk about pure magnesium implants that perform their functions independently, based on this work, we can conclude that direct contact with titanium products in the human body threatens the failure of the implant, before the completion of the fusion process. In one of our previous works, it was found that when a titanium implant is located 3 cm from a sample made of ZX10 alloy, the corrosion rate increases by 1.5 times, but at a distance of 6 cm this effect completely disappears [11]. This shows that the electrochemical interaction between magnesium and titanium, can manifest itself both in direct contact of metals and at some distance, and that the influence of this effect on the corrosion rate is significant.

Another important parameter is the ratio of the areas of magnesium and titanium alloy products. The main hypothesis is that, an increase in the area of a magnesium product relative to a titanium one, can reduce to some extent the influence of the electrochemical effect on the corrosion rate. Confirmation of this hypothesis will allow the installation of a large magnesium implant, such as an osteosynthesis plate, near a small titanium implant, such as a screw. Finally, it is important to understand whether the galvanic effect is equally strong for different magnesium alloys. Considering that it is caused by the difference in electrode potentials, it can be assumed that for alloys with a large number of secondary phase particles whose potential is more positive than that of magnesium, or a matrix whose electrode potential has been increased by dissolving alloying elements in it, the influence of electrochemical interaction with the titanium alloy will be significantly weaker. In this regard, this study was conducted for two different magnesium alloys.

The aim of the work is to determine the influence of the ratio of the areas of samples of ZX10 and WZ31 magnesium alloys, and a sample of Ti6Al4V titanium alloy on the corrosion rate.

METHODS

Bioresorbable ZX10 and WZ31 alloys were selected for the study. Multi-axial isothermal forging was selected as the thermomechanical treatment, which was carried out in the temperature range of 400–300 °C, and included 5 passes. This treatment mode ensures a uniform fine-grained structure [12]. The chemical composition of magnesium alloys was determined using a Thermo Fisher Scientific ARL 4460 OES optical emission spectrometer (USA). The chemical composition of the titanium alloy was determined on a Bruker Q4 Tasman optical emission spectrometer (Germany). Both spectrometers were calibrated using standard samples.

The samples (including those made of titanium alloy) were cylinders with a diameter of 5 mm and a height of 30 mm prepared by turning. The titanium Ti6Al4V alloy used in the study complied with GOST R ISO 5832-3-2020. Separately, flat samples were made to study the microstructure of the ZX10 and WZ31 alloys, which were successively polished on anhydrous diamond suspensions with an abrasive size of 3, 1 and 0.25 μm, followed by ion polishing in an argon ion stream on a Hitachi IM4000 Plus installation (Japan) at an accelerating voltage of 4.5 kV for 45 min.

The microstructure study was carried out in a Carl Zeiss SIGMA scanning electron microscope (SEM) column (Germany), using EDAX modules (USA), for electron backscatter diffraction (EBSD) and energy-dispersive spectrometry (EDS) analysis. The WZ31 alloy had a large number of secondary phase particles, whose electrode potential was additionally studied using the Kelvin probe method using an NT-MDT Solver NEXT atomic force microscope (Russia).

The corrosion tests included keeping the sample for 72 h in a Ringer solution of 8.36 g of NaCl, 0.3 g of KCl, and 0.15 g of $CaCl_2$ per 1000 ml of water. The volume of the corrosion cell was 5 l. A Mettler Toledo Delta 320 pH-meter (USA) was used to record the maximum pH level. Tests of the control group (in the absence of titanium alloy) were performed on samples of both alloys. The initial corrosion rate was determined for one and for four samples simultaneously participating in the experiment, since the number of samples in the cell could affect the corrosion rate. During the main series of experiments, the titanium rod was fixed in a groove in the middle of a fluoroplastic washer with a diameter of 7 cm. Grooves for installing magnesium alloy samples were located in a circle at a radius of 3 cm from it. Fig. 1 shows the setup diagram. One, two and four magnesium alloy samples were used in the experiment at a time, so the ratio of the areas of the titanium and magnesium alloys was 1:1, 1:2 and 1:4.

After the tests were completed, the samples were removed, and the corrosion products were removed by immersion for 1 min in an aqueous solution of 20 % CrO_3 + +1 % $AgNO_3$. The corrosion rate was determined gravimetrically by the difference in masses.

RESULTS

Table 1 shows the chemical composition of magnesium alloys. Table 2 shows the chemical composition of a titanium alloy.

Fig. 2 shows that the ZX10 alloy has an average grain size of about 5 μm, while the WZ31 alloy has an average grain size of about 1 μm. Both alloys have a disordered structure and no crystallographic texture, which is typical of alloys after multi-axial isothermal forging. This allows avoiding the anisotropy of corrosion properties, caused by crystallographic orientation, which is observed in highly textured materials. Dark areas corresponding to non-indexed regions are visible in Fig. 2 b.

Secondary phase particles in the ZX10 alloy are few in number, and contain zinc and calcium (Fig. 3). Based on the elemental composition, the phase with spongy morphology in the ZX10 alloy (point 1 in Fig. 3) is most likely calcium, and magnesium oxide particles. Particles at points 2 and 3 are most likely intermetallides formed by the matrix metal and alloying elements.

In contrast, the WZ31 alloy is saturated with particles mostly having a morphology characteristic of the LPSO phase (Fig. 4). In addition to large (up to 15 μm) LPSO phase particles, there are small particles 0.2–2 μm in size. Most likely, the small particles were obtained by mechanical crushing of large ones during thermomechanical treatment. The elemental composition of the LPSO phase is shown in Table 3.

The results of the Kelvin probe study of the WZ31 alloy presented in Fig. 5 show both large and small particles, positively charged relative to the matrix, presumably representing the LPSO phase.

Fig. 6 demonstrates that for both magnesium alloys the corrosion rate in the presence of titanium alloy is higher than during the tests of the control group. However, it should be noted that the difference depends significantly on both the chemical composition of the material and the number of anodes (magnesium samples), and accordingly, on the ratio of the areas of magnesium and titanium alloys: with an increase in the number of magnesium alloys, their corrosion rate decreases.

Table 4 shows the maximum pH level found for each group of samples during the experiments. One should note that in all cases, regardless of the presence of titanium alloy and the number of anodes, the pH level reaches its maximum values in the first day, and then remains virtually unchanged.

DISCUSSION

The presence of the LPSO phase is indirectly confirmed by the results of EBSD analysis: according to the literature, the dark non-indexed areas in Fig. 2 b correspond to the LPSO phase [13; 14].

Based on the elemental composition, the phase with a spongy morphology in the ZX10 alloy (point 1 in Fig. 3) is most likely particles of calcium and magnesium oxides, while the rounded particles (points 2 and 3 in Fig. 3) have a ratio of zinc atoms to calcium atoms of ~2.2. Due to this, they most likely belong to the $Ca_2Mg_5Zn_5$ [15] and $Mg_6Zn_3Ca_2$ [16] phases.

The chemical composition of the LPSO phase in the studied WZ31 alloy is very close to that presented in the literature [17]. It is known that the LPSO phase is more positively charged than the matrix. A study using Kelvin probe atomic force microscopy (Fig. 4), allowed determining that the electrode potential of the LPSO phase (light areas in Fig. 4) in the WZ31 alloy is really 0.3–0.4 V more positive than the matrix, which is fully consistent with the results of [18; 19].

Based on the results of the experiments, several important facts can be noted. Firstly, regardless of the material and number of magnesium samples, the corrosion rate in the presence of the titanium alloy is always higher than without it, i.e. in all cases a galvanic effect occurred between the titanium and magnesium alloys.

The second important result is that the dependence of the corrosion rate on the ratio of the areas of the titanium and magnesium alloys differs significantly for the ZX10 and WZ31 alloys. If for the ZX10 alloy an increase in the area ratio from 1:1 to 1:2 provokes a sharp decrease in the corrosion rate, which gives the curve the appearance of a hyperbola, then for the WZ31 alloy the curve has rather the appearance of a straight line along its entire length (Fig. 6). Moreover, the difference between the corrosion rate of the samples in the presence of the titanium alloy and the samples of the control group is smaller for this alloy. From this, we can conclude that the WZ31 alloy is less sensitive to the galvanic effect caused by the presence of the titanium alloy. This is well explained by the fact that the WZ31 matrix contains zinc and yttrium dissolved in it, due to which its electrode potential is increased, as well as by the presence in the alloy of a large number of LPSO phase particles, which are more positively charged than magnesium. Thus, the difference in electrode potentials between WZ31 and Ti6Al4V is smaller than between Ti6Al4V and ZX10.

An interesting result is the decrease in the corrosion rate of the control samples with an increase in the number of anodes observed for both alloys. This effect can be

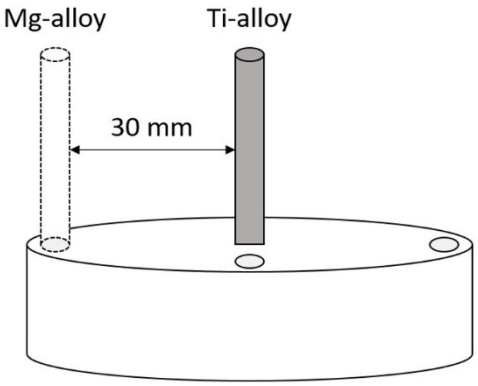

Fig. 1. *Schematic diagram of the arrangement of samples during the corrosion tests*
Рис. 1. *Схема расположения образцов во время коррозионных испытаний*

Table 1. *Chemical composition of the WZ31 and ZX10 magnesium alloys, % wt.*
Таблица 1. *Химический состав магниевых сплавов WZ31 и ZX10, вес. %*

Alloy	Mg	Zn	Zr	Ca	Fe	Mn	Si	Al	Cu	Y
WZ31	Base	0.69	0.13	<0.001	0.004	0.002	0.002	0.008	<0.001	2.790
ZX10		1.48	<0.01	0.098	0.004	0.003	0.002	0.010	<0.001	<0.001

Table 2. *Chemical composition of the Ti6Al4V alloy, % wt.*
Таблица 2. *Химический состав сплава Ti6Al4V, вес. %*

Ti	Si	Mn	Cr	Ni	Mo	Al	Fe	V	C	Cu
Base	0.016	0.002	0.021	0.011	0.011	5.618	0.102	3.950	<0.002	0.006

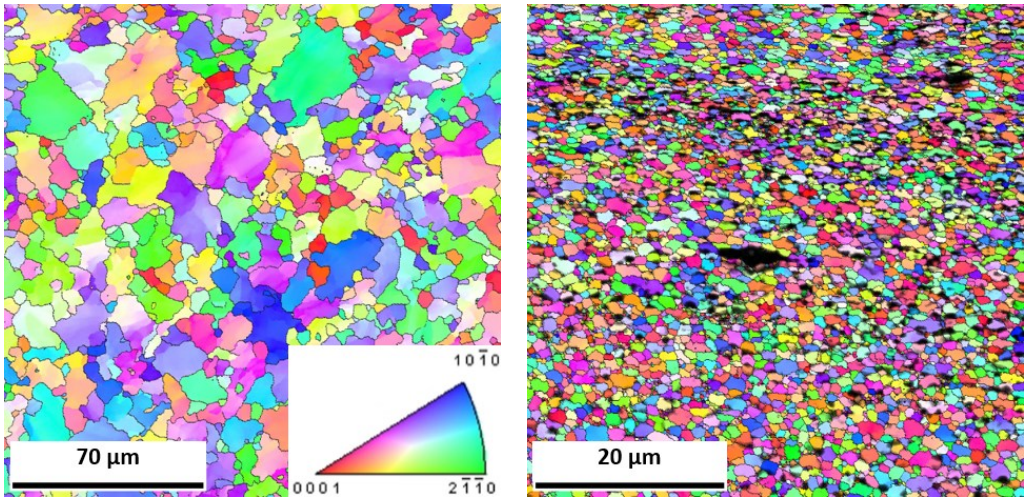

a ***b***

Fig. 2. *Maps of crystallographic orientations of grains of the ZX10 (**a**) and WZ31 (**b**) alloys*
Рис. 2. *Карта кристаллографических ориентаций зерен сплавов ZX10 (**a**) и WZ31 (**b**)*

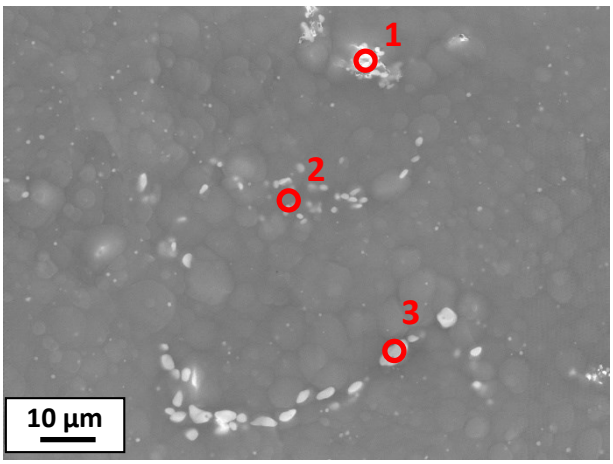

Spot	Ca (at.%)	Zn (at.%)	O (at.%)
1	8.97	3.17	21.11
2	7.32	16.09	-
3	4.41	9.83	-

Fig. 3. *SEM image and chemical composition of secondary phase particles in the ZX10 alloy*
Рис. 3. *СЭМ-снимок и химический состав частиц вторичных фаз в сплаве ZX10*

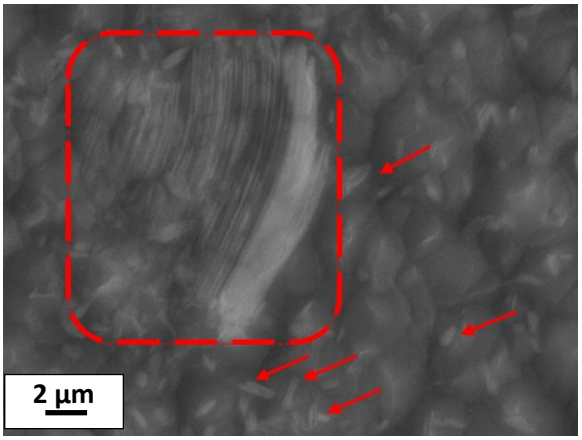

Fig. 4. *LPSO phase particles (marked by red arrows and frame) in the WZ31 alloy*
Рис. 4. *Частицы LPSO-фазы (помечены красными стрелками и рамкой) в сплаве WZ31*

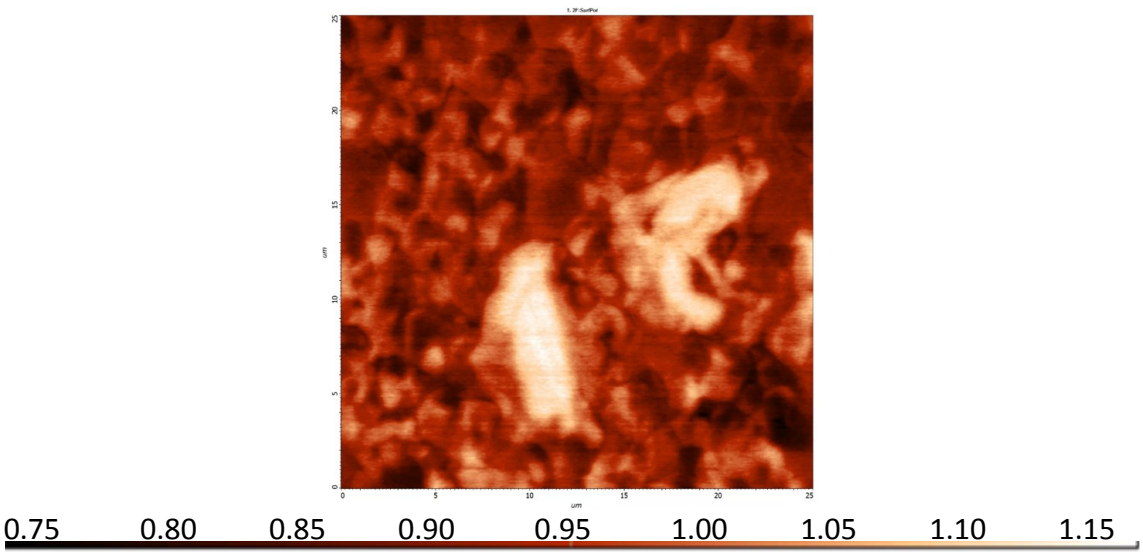

Fig. 5. *Electrode potential distribution on the WZ31 alloy surface. Light areas are the LPSO phase*
Рис. 5. *Распределение электродного потенциала на поверхности сплава WZ31. Светлые участки – LPSO-фаза*

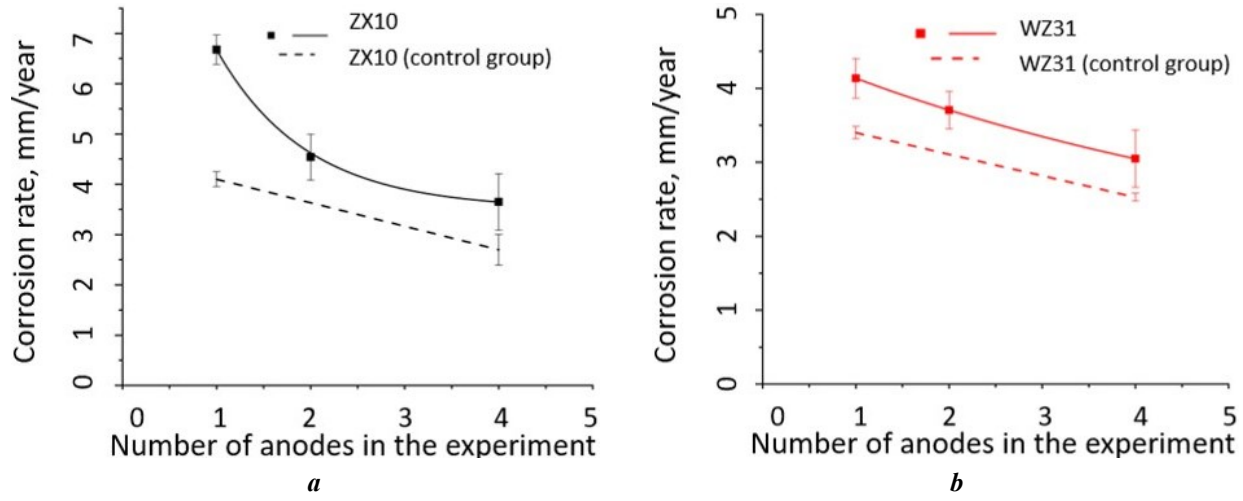

Fig. 6. *Dependence of the corrosion rate of the ZX10 (**a**) and WZ31 (**b**) alloys on the number of magnesium alloy samples (anodes)*
Рис. 6. *Зависимость скорости коррозии сплавов ZX10 (**a**) и WZ31 (**b**) от числа образцов магниевого сплава (анодов)*

Table 3. *Chemical composition of the WZ31 alloy matrix and LPSO phase*
Таблица 3. *Химический состав матрицы сплава WZ31 и его LPSO-фазы*

Area	Mg (wt. %)	Y (wt. %)	Zn (wt. %)	Mg (at. %)	Y (at. %)	Zn (at. %)
Matrix	96.65	2.43	0.92	98.97	0.68	0.35
LPSO phase	74.5	17.33	8.17	90.55	5.76	3.69

Table 4. *Maximum pH level of the solution achieved during corrosion tests*
Таблица 4. *Максимальный уровень pH раствора, достигнутый в ходе коррозионных испытаний*

Group of samples	Maximum pH level
ZX10 control group, 1 anode	8.52
ZX10 control group, 4 anodes	9.44
ZX10, 1 anode	8.52
ZX10, 2 anodes	8.68
ZX10, 4 anodes	9.39
WZ31 control group, 1 anode	8.32
WZ31 control group, 4 anodes	9.21
WZ31, 1 anode	8.23
WZ31, 2 anodes	8.46
WZ31, 4 anodes	9.24

explained by a significantly higher maximum pH level of the solution in the experiments involving four anodes, which is consistent with the results of [20], where it was shown that at a high pH level, the corrosion of the magnesium AZ31 alloy slows down. In all such cases, the pH level during the first day took a value of about 9.2–9.4, after which its growth stopped. It was previously demonstrated that a high pH level could contribute to better passivation of the surface of the ZX10 alloy [21]. Apparently, a similar feature is characteristic of WZ31.

CONCLUSIONS

1. Increasing the area ratio of the ZX10 and Ti6Al4V alloy samples from 1:1 to 1:2 leads to a sharp drop in the corrosion rate. Increasing the area ratio from 1:2 to 1:4 also contributes to a decrease in the corrosion rate, but not as significantly.

2. The corrosion rate of the WZ31 alloy decreases almost linearly, with an increase in the area ratio of the ZX10 and Ti6Al4V alloy samples.

3. The WZ31 alloy is less sensitive to the galvanic effect introduced by the presence of a titanium alloy at a distance of 3 cm. This is explained by an increase in the electrode potential of the matrix, due to the dissolution of alloying elements in it and the presence of a large amount of the LPSO phase.

4. Increasing the number of magnesium samples in the control group from 1 to 4 also leads to a decrease in the corrosion rate of both alloys under study. The most likely cause of this phenomenon is a significantly higher maximum pH level of the solution, which can contribute to better passivation of the material.

REFERENCES

1. Antoniac I., Popescu D., Zapciu A., Antoniac A., Miculescu F., Moldovan H. Magnesium filled polylactic acid (PLA) material for filament based 3D printing. *Materials (Basel)*, 2019, vol. 12, no. 5, pp. 1–13. DOI: 10.3390/ma12050719.
2. Yang Youwen, He Chongxian, E Dianyu, Yang Wenjing, Qi Fangwei, Xie Deqiao, Shen Lida, Peng Shuping, Shuai Cijun. Mg bone implant: Features, developments and perspectives. *Materials and Design*, 2020, vol. 185, article number 108259. DOI: 10.1016/j.matdes.2019.108259.
3. Butler T.J., Jackson R.W., Robson J.Y., Owen R.J.T., Delves H.T., Sieniawska C.E., Rose J.D.G. In vivo degradation of tungsten embolisation coils. *British Journal of Radiology*, 2000, vol. 73, no. 870, pp. 601–603. DOI: 10.1259/bjr.73.870.10911782.
4. Peuster M., Fink C., Wohlsein P., Bruegmann M., Günther A., Kaese V., Niemeyer M., Haferkamp H., Schnakenburg C.V. Degradation of tungsten coils implanted into the subclavian artery of New Zealand white rabbits is not associated with local or systemic toxicity. *Biomaterials*, 2003, vol. 24, no. 3, pp. 393–399. DOI: 10.1016/S0142-9612(02)00352-6.
5. Zheng Y.F., Gu X.N., Witte F. Biodegradable metals. *Materials Science and Engineering: R: Reports*, 2014, vol. 77, pp. 1–34. DOI: 10.1016/j.mser.2014.01.001.
6. Song G.-L. Corrosion electrochemistry of magnesium (Mg) and its alloys. *Corrosion of Magnesium Alloys*. Sawston, Woodhead Publ., 2011, pp. 3–65. DOI: 10.1533/9780857091413.1.3.
7. Esmaily M., Svensson J.E., Fajardo S., Birbilis N., Frankel G.S., Virtanen S., Arrabal R., Thomas S., Johansson L.G. Fundamentals and advances in magnesium alloy corrosion. *Progress in Materials Science*, 2017, vol. 89, pp. 92–193. DOI: 10.1016/j.pmatsci.2017.04.011.
8. Parfenov E.V., Kulyasova O.B., Mukaeva V.R., Mingo B., Farrakhov R.G., Cherneikina Y.V., Yerokhin A., Zheng Y.F., Valiev R.Z. Influence of ultra-fine grain structure on corrosion behaviour of biodegradable Mg-1Ca alloy. *Corrosion Science*, 2020, vol. 163, article number 108303. DOI: 10.1016/j.corsci.2019.108303.
9. Ma Yingzhong, Wang Dexin, Li Hongxiang, Yuan Fusong, Yang Changlin, Zhang Jishan. Microstructure, mechanical and corrosion properties of novel quaternary biodegradable extruded Mg-1Zn-0.2Ca-xAg alloys. *Materials Research Express*, 2020, vol. 7, no. 1, article number 015414. DOI: 10.1088/2053-1591/ab6a52.
10. Tian Li, Sheng Yifeng, Huang Le et al. An innovative Mg/Ti hybrid fixation system developed for fracture fixation and healing enhancement at load-bearing skeletal site. *Biomaterials*, 2018, vol. 180, pp. 173–183. DOI: 10.1016/j.biomaterials.2018.07.018.
11. Myagkikh P.N., Merson E.D., Poluyanov V.A., Merson D.L., Begun M.E. On the compatibility of surgical implants of bioresorbable magnesium alloys with medical devices of titanium alloys. *Frontier Materials & Technologies*, 2022, no. 3-1, pp. 106–114. DOI: 10.18323/2782-4039-2022-3-1-106-114.
12. Merson D.L., Brilevsky A.I., Myagkikh P.N., Markushev M.V., Vinogradov A. Effect of deformation processing of the dilute Mg–1Zn–0.2Ca alloy on the mechanical properties and corrosion rate in a simulated body fluid. *Letters on Materials*, 2020, vol. 10, no. 2, pp. 217–222. DOI: 10.22226/2410-3535-2020-2-217-222.
13. Myagkikh P.N., Merson E.D., Poluyanov V.A., Merson D.L. Structure effect on the kinetics and staging of the corrosion process of biodegradable ZX10 and WZ31 magnesium alloys. *Frontier Materials & Technologies*, 2022, no. 2, pp. 63–73. DOI: 10.18323/2782-4039-2022-2-63-73.
14. Zheng Jie, Chen Zhe, Yan Zhaoming, Zhang Zhimin, Wang Qiang, Xue Yong. Preparation of ultra-high strength Mg–Gd–Y–Zn–Zr alloy by pre-ageing treatment prior to extrusion. *Journal of Alloys and Compounds*, 2022, vol. 894, article number 162490. DOI: 10.1016/j.jallcom.2021.162490.
15. Schäublin R.E., Becker M., Cihova M., Gerstl S.S.A., Deiana D., Hébert C., Pogatscher S., Uggowitzer P.J., Löffler J.F. Precipitation in lean Mg–Zn–Ca alloys. *Acta Materialia*, 2022, vol. 239, article number 118223. DOI: 10.1016/j.actamat.2022.118223.
16. Martynenko N., Anisimova N., Kiselevskiy M. et al. Structure, mechanical characteristics, biodegradation, and in vitro cytotoxicity of magnesium alloy ZX11 processed by rotary swaging. *Journal of Magnesium and Alloys*, 2020, vol. 8, no. 4, pp. 1038–1046. DOI: 10.1016/j.jma.2020.08.008.
17. Liu Shimeng, Wei Ziqi, Liu Zheng, Mao Pingli, Wang Feng, Wang Zhi, Zhou Le, Yin Xiunan. Effect of Zn content on hot tearing susceptibility of LPSO enhanced Mg–Zn_x–Y_2–$Zr_{0.06}$ alloys with different initial mold temperatures. *Journal of Alloys and Compounds*, 2022, vol. 904, article number 163963. DOI: 10.1016/j.jallcom.2022.163963.
18. Li C.Q., Xu D.K., Zeng Z.R., Wang B.J., Sheng L.Y., Chen X.B., Han E.H. Effect of volume fraction of LPSO phases on corrosion and mechanical properties of Mg–Zn–Y alloys. *Materials and Design*, 2017, vol. 121, pp. 430–441. DOI: 10.1016/j.matdes.2017.02.078.

19. Zong Ximei, Zhang Jinshan, Liu Wei, Zhang Yatong, You Zhiyong, Xu Chunxiang. Corrosion Behaviors of Long-Period Stacking Ordered Structure in Mg Alloys Used in Biomaterials: A Review. *Advanced Engineering Materials*, 2018, vol. 20, no. 7, pp. 1–26. DOI: 10.1002/adem.201800017.
20. Azzeddine H., Hanna A., Dakhouche A. Exploring the Corrosion Performance of AZ31 Magnesium Alloy under Acidic and Alkaline Conditions. *Physics of Metals and Metallography*, 2024, pp. 1–8. DOI: 10.1134/S0031918X24600258.
21. Myagkikh P.N., Merson E.D., Poluyanov V.A., Merson D.L. The dependence of the biodegradable ZX10 alloy corrosion process on the structural factors and local pH level. *Frontier Materials & Technologies*, 2023, no. 2, pp. 59–76. DOI: 10.18323/2782-4039-2023-2-64-3.

СПИСОК ЛИТЕРАТУРЫ

1. Antoniac I., Popescu D., Zapciu A., Antoniac A., Miculescu F., Moldovan H. Magnesium filled polylactic acid (PLA) material for filament based 3D printing // Materials (Basel). 2019. Vol. 12. № 5. P. 1–13. DOI: 10.3390/ma12050719.
2. Yang Youwen, He Chongxian, E Dianyu, Yang Wenjing, Qi Fangwei, Xie Deqiao, Shen Lida, Peng Shuping, Shuai Cijun. Mg bone implant: Features, developments and perspectives // Materials and Design. 2020. Vol. 185. Article number 108259. DOI: 10.1016/j.matdes.2019.108259.
3. Butler T.J., Jackson R.W., Robson J.Y., Owen R.J.T., Delves H.T., Sieniawska C.E., Rose J.D.G. In vivo degradation of tungsten embolisation coils // British Journal of Radiology. 2000. Vol. 73. № 870. P. 601–603. DOI: 10.1259/bjr.73.870.10911782.
4. Peuster M., Fink C., Wohlsein P., Bruegmann M., Günther A., Kaese V., Niemeyer M., Haferkamp H., Schnakenburg C.V. Degradation of tungsten coils implanted into the subclavian artery of New Zealand white rabbits is not associated with local or systemic toxicity // Biomaterials. 2003. Vol. 24. № 3. P. 393–399. DOI: 10.1016/S0142-9612(02)00352-6.
5. Zheng Y.F., Gu X.N., Witte F. Biodegradable metals // Materials Science and Engineering: R: Reports. 2014. Vol. 77. P. 1–34. DOI: 10.1016/j.mser.2014.01.001.
6. Song G.-L. Corrosion electrochemistry of magnesium (Mg) and its alloys // Corrosion of Magnesium Alloys. Sawston: Woodhead Publishing, 2011. P. 3–65. DOI: 10.1533/9780857091413.1.3.
7. Esmaily M., Svensson J.E., Fajardo S., Birbilis N., Frankel G.S., Virtanen S., Arrabal R., Thomas S., Johansson L.G. Fundamentals and advances in magnesium alloy corrosion // Progress in Materials Science. 2017. Vol. 89. P. 92–193. DOI: 10.1016/j.pmatsci.2017.04.011.
8. Parfenov E.V., Kulyasova O.B., Mukaeva V.R., Mingo B., Farrakhov R.G., Cherneikina Y.V., Yerokhin A., Zheng Y.F., Valiev R.Z. Influence of ultra-fine grain structure on corrosion behaviour of biodegradable Mg-1Ca alloy // Corrosion Science. 2020. Vol. 163. Article number 108303. DOI: 10.1016/j.corsci.2019.108303.
9. Ma Yingzhong, Wang Dexin, Li Hongxiang, Yuan Fusong, Yang Changlin, Zhang Jishan. Microstructure, mechanical and corrosion properties of novel quaternary biodegradable extruded Mg-1Zn-0.2Ca-xAg alloys // Materials Research Express. 2020. Vol. 7. № 1. Article number 015414. DOI: 10.1088/2053-1591/ab6a52.
10. Tian Li, Sheng Yifeng, Huang Le et al. An innovative Mg/Ti hybrid fixation system developed for fracture fixation and healing enhancement at load-bearing skeletal site // Biomaterials. 2018. Vol. 180. P. 173–183. DOI: 10.1016/j.biomaterials.2018.07.018.
11. Мягких П.Н., Мерсон Е.Д., Полуянов В.А., Мерсон Д.Л., Бегун М.Э. О совместимости хирургических имплантатов из биорезорбируемых магниевых сплавов с медицинскими изделиями из титановых сплавов // Frontier Materials & Technologies. 2022. № 3-1. С. 106–114. DOI: 10.18323/2782-4039-2022-3-1-106-114.
12. Merson D.L., Brilevsky A.I., Myagkikh P.N., Markushev M.V., Vinogradov A. Effect of deformation processing of the dilute Mg–1Zn–0.2Ca alloy on the mechanical properties and corrosion rate in a simulated body fluid // Letters on Materials. 2020. Vol. 10. № 2. P. 217–222. DOI: 10.22226/2410-3535-2020-2-217-222.
13. Мягких П.Н., Мерсон Е.Д., Полуянов В.А., Мерсон Д.Л. Влияние структуры на кинетику и стадийность процесса коррозии биорезорбируемых магниевых сплавов ZX10 и WZ31 // Frontier Materials & Technologies. 2022. № 2. С. 63–73. DOI: 10.18323/2782-4039-2022-2-63-73.
14. Zheng Jie, Chen Zhe, Yan Zhaoming, Zhang Zhimin, Wang Qiang, Xue Yong. Preparation of ultra-high strength Mg–Gd–Y–Zn–Zr alloy by pre-ageing treatment prior to extrusion // Journal of Alloys and Compounds. 2022. Vol. 894. Article number 162490. DOI: 10.1016/j.jallcom.2021.162490.
15. Schäublin R.E., Becker M., Cihova M., Gerstl S.S.A., Deiana D., Hébert C., Pogatscher S., Uggowitzer P.J., Löffler J.F. Precipitation in lean Mg–Zn–Ca alloys // Acta Materialia. 2022. Vol. 239. Article number 118223. DOI: 10.1016/j.actamat.2022.118223.
16. Martynenko N., Anisimova N., Kiselevskiy M. et al. Structure, mechanical characteristics, biodegradation, and in vitro cytotoxicity of magnesium alloy ZX11 processed by rotary swaging // Journal of Magnesium and Alloys. 2020. Vol. 8. № 4. P. 1038–1046. DOI: 10.1016/j.jma.2020.08.008.
17. Liu Shimeng, Wei Ziqi, Liu Zheng, Mao Pingli, Wang Feng, Wang Zhi, Zhou Le, Yin Xiunan. Effect of Zn content on hot tearing susceptibility of LPSO enhanced Mg–Zn_x–Y_2–$Zr_{0.06}$ alloys with different initial mold temperatures // Journal of Alloys and Compounds. 2022. Vol. 904. Article number 163963. DOI: 10.1016/j.jallcom.2022.163963.
18. Li C.Q., Xu D.K., Zeng Z.R., Wang B.J., Sheng L.Y., Chen X.B., Han E.H. Effect of volume fraction of LPSO phases on corrosion and mechanical properties of Mg–Zn–Y alloys // Materials and Design. 2017. Vol. 121. P. 430–441. DOI: 10.1016/j.matdes.2017.02.078.
19. Zong Ximei, Zhang Jinshan, Liu Wei, Zhang Yatong, You Zhiyong, Xu Chunxiang. Corrosion Behaviors of Long-Period Stacking Ordered Structure in Mg Alloys Used in Biomaterials: A Review // Advanced Engineering Materials. 2018. Vol. 20. № 7. P. 1–26. DOI: 10.1002/adem.201800017.

20. Azzeddine H., Hanna A., Dakhouche A. Exploring the Corrosion Performance of AZ31 Magnesium Alloy under Acidic and Alkaline Conditions // Physics of Metals and Metallography. 2024. P. 1–8. DOI: 10.1134/S0031918X24600258.

21. Мягких П.Н., Мерсон Е.Д., Полуянов В.А., Мерсон Д.Л. Зависимость процесса коррозии биорезорбируемого сплава ZX10 от структурных факторов и локального уровня pH // Frontier Materials & Technologies. 2023. № 2. С. 59–76. DOI: 10.18323/2782-4039-2023-2-64-3.

Электрохимическое взаимодействие между биорезорбируемыми магниевыми сплавами ZX10 и WZ31 и медицинским титановым сплавом Ti6Al4V

Мягких Павел Николаевич*[1], кандидат технических наук,
младший научный сотрудник НИИ прогрессивных технологий
Мерсон Евгений Дмитриевич[2], кандидат физико-математических наук,
старший научный сотрудник НИИ прогрессивных технологий
Полуянов Виталий Александрович[3], кандидат технических наук,
младший научный сотрудник НИИ прогрессивных технологий
Мерсон Дмитрий Львович[4], доктор физико-математических наук,
профессор, директор НИИ прогрессивных технологий
Бегун Марина Эдуардовна, студент, техник НИИ прогрессивных технологий
Тольяттинский государственный университет, Тольятти (Россия)

***E-mail:** p.myagkikh@tltsu.ru

[1]ORCID: https://orcid.org/0000-0002-7530-9518
[2]ORCID: https://orcid.org/0000-0002-7063-088X
[3]ORCID: https://orcid.org/0000-0002-0570-2584
[4]ORCID: https://orcid.org/0000-0001-5006-4115

Поступила в редакцию 08.05.2024 *Пересмотрена 09.10.2024* *Принята к публикации 07.11.2024*

Аннотация: Сплавы на основе магния являются современным материалом для изготовления биорезорбируемых (саморастворяющихся) хирургических имплантатов. Магний – металл с наиболее отрицательным из всех конструкционных материалов электродным потенциалом −2,37 В. Это означает, что близкое расположение имплантатов из магниевых и, например, титановых сплавов будет приводить к возникновению гальванического эффекта и ускоренной электрохимической коррозии магния. Однако неизвестно, как влияет соотношение площадей изделий из титана и магния на проявление этого эффекта. Данная работа посвящена этому вопросу. В приведенном исследовании цилиндрические образцы биорезорбируемых магниевых сплавов ZX10 и WZ31 располагались в физиологическом растворе Рингера на расстоянии 3 см от образца из сплава медицинского назначения Ti6Al4V такой же формы и размера. Во время испытания поддерживалась температура коррозионной среды 37 °C. Серия экспериментов включала в себя коррозионные испытания длительностью трое суток с участием одного, двух или четырех магниевых образцов, таким образом, соотношение площадей титанового и магниевого сплава составляло 1:1, 1:2 и 1:4. Выявлено, что для обоих магниевых сплавов при увеличении соотношения площадей эффект от электрохимического воздействия значительно снижается, что выражено в уменьшении скорости коррозии. В то же время влияние присутствия Ti6Al4V на скорость коррозии для сплава WZ31 существенно слабее, чем для ZX10, что объясняется наличием в сплаве LPSO-фазы, а также более легированной и, соответственно, имеющей более положительный электродный потенциал матрицей.

Ключевые слова: хирургические имплантаты; электрохимическая коррозия; биорезорбируемые материалы; магниевые сплавы; ZX10; WZ31; титановые сплавы; Ti6Al4V; медицинские материалы; скорость коррозии; электродный потенциал.

Благодарности: Исследование выполнено при финансовой поддержке Российского научного фонда, проект № 23-23-10041 (https://rscf.ru/project/23-23-10041/), проект № 23-19-00636 (https://rscf.ru/project/23-19-00636/).

Для цитирования: Мягких П.Н., Мерсон Е.Д., Полуянов В.А., Мерсон Д.Л., Бегун М.Э. Электрохимическое взаимодействие между биорезорбируемыми магниевыми сплавами ZX10 и WZ31 и медицинским титановым сплавом Ti6Al4V // Frontier Materials & Technologies. 2024. № 4. С. 63–71. DOI: 10.18323/2782-4039-2024-4-70-6.